Electrical Power and Energy Systems 137 (2022) 107825

Contents lists available at ScienceDirect

International Journal of Electrical Power and Energy Systems

journal homepage: www.elsevier.com/locate/ijepes

Fault detection in a power transformer based on reverberation time

Milos Bjelić, Bogdan Brković *, Mileta Žarković, Tatjana Miljković

University of Belgrade, School of Electrical Engineering, Bulevar kralja Aleksandra 73, 11000 Belgrade, Serbia

ARTICLE INFO

Keywords:
Power transformer
Fault detection
Winding defects
Reverberation time
Signal processing

ABSTRACT

The power transformer is one of the vital elements of electric power systems. The reliability of power transformer operation is directly related to its condition. Detection of winding deformations is possible by means of sweep frequency response analysis. Interpretation of SFRA results is usually performed by visualization of images generated using specialized devices and comparison of transfer functions obtained from successive tests. This diagnostic method is known as a fingerprint and its disadvantage is the subjectivity and relying on engineer's experience. This paper presents an experimental approach for detection of internal transformer short-circuit faults. Existing mathematical indicators based on frequency response analysis are often unable to unambiguously indicate the degree of fault and their determination requires high-cost measurement and signal processing equipment. A new indicator based on the reverberation time, commonly employed in acoustics, is proposed instead. The proposed parameter is based on time-domain calculation and enables reliable detection of transformer inter-turn short circuits and accurate estimation of their degree. A significant advantage of the proposed approach is its low dependence on the frequency range of the measured signal, which allows employment of low-cost measuring and signal processing devices.

1. Introduction

A power transformer (PT) is vital for the transmission and distribution of electrical energy. It is also one of the most expensive elements in every part and at every voltage level of the electric power system (EPS). Additionally, the PT is a highly complex and heterogeneous component whose operation is influenced by thermal, mechanical, electrical, and chemical processes. For these reasons, considerable attention is dedicated to monitoring and diagnostics of PT. The investment in diagnostics and monitoring is incomparable with the price of the device itself; therefore, great efforts are made to ensure timely and proper maintenance to extend the life of the PT. Some of the key parts of a transformer that are of great importance for its reliable operation are: magnetic circuit, oil, windings (state of geometry and state of electrical connections), and solid insulation of windings. Winding deformations can occur due to prolonged stress during normal operation, whereas during short circuits strong dynamic forces can lead to permanent, plastic deformations. Winding deformations are usually detected using frequency response analysis (FRA) method and sweep frequency response analysis (SFRA). The standard SFRA method involves comparing the frequency responses of consecutive periodically conducted tests. If the two compared frequency responses do not differ, then the longitudinal R, L and C parameters did not change significantly, indicating that no deformations occurred in the meantime. Interpretation of SFRA results is usually done by visualization of images generated by specialized devices for such testing. The frequency response most often does not provide sufficient information, which is why transfer functions need to be obtained for each test. The transfer function represents the ratio of the input, test signal, and the output signal, i.e., the recorded response on the PT. By comparing the generated transfer functions from successive tests, changes in the geometry of the winding or the magnetic circuit of a PT can be detected.

The papers and standards [1]–[13] present the FRA and SFRA method and its importance in PT monitoring and diagnostics. Reference [1] presents theoretical foundations of the FRA method and its application to signals recorded during PT exploitation. The development of vibration – acoustic methods was presented in [2], where an attempt was made to supplement the results of the FRA method and correlate it to existing IEEE standards [3], IEC standard [4] and the experience of the CIGRE working group [5,6]. A good interpretation of the results of the FRA method is presented in [7], where an attempt was made to determine individual quantifiers and their approximate limit values. The presented quantifiers were calculated in this paper for the results of the experiments. The method that clusters the simulation results of the FRA

* Corresponding author.
E-mail address: brkovic@etf.rs (B. Brković).

https://doi.org/10.1016/j.ijepes.2021.107825
Received 1 July 2021; Received in revised form 20 September 2021; Accepted 20 November 2021

method and connects them with a certain type of failure is presented in [8]. The experiments of PT in idle and short-circuit conditions with the application of the FRA method are presented in [9]. The detection of radial winding deformation using lightning impulse voltage is present in [10]. Common statistical fault indicators are calculated in [11,12,13]. None of the papers included a representation of all indicators for different faults that were obtained both in laboratory conditions and from actual periodic measurements on PTs in exploitation. An approach for winding deformation detection using a time–frequency image of the frequency response is proposed in [14]. Reference [15] presents a new methodology for PT diagnostics based on SFRA results and [16] compares finite element method with FRA in terms of detection of internal and external short-circuit faults. More recently, artificial intelligence (AI)–based methods have been proposed for detecting and differentiating winding deformations [17].

Interpretation of SFRA results is usually performed visually, based on images generated by dedicated measuring devices. Development of new methods is motivated by the need to achieve objective interpretation of results and to improve the processing and interpretation of SFRA method results. This paper summarizes all identifiers obtained from SFRA tests. Such identifiers should more clearly quantify the results of the SFRA method and allow easier and unambiguous detection of PT winding and magnetic circuit failures.

In this paper, detection of inter-turn short circuits and determining their severity is performed using reverberation time. Reverberation time is a parameter typically used in acoustics and signal processing [18]. This parameter is most commonly used for quantification of room acoustics. The main hypothesis of the research is that the number of short-circuited turns can be determined based on the value of reverberation time. To validate this hypothesis, two sets of measurements are performed. Both sets of experiments include short-circuiting different parts of one PT winding while exciting a different winding using a signal of variable frequency. The first set of measurements is a reference set obtained using a professional SFRA analyzer. The second set of measurements is conducted using an audio card with a considerably lower bandwidth compared to the SFRA analyzer. Results from the second set are compared to those from the first (reference) set to verify the possibility of using a low-cost audio card instead of the expensive SFRA analyzer. Additionally, the recorded signals are used to calculate statistical parameters commonly used in literature for PT fault detection. A comparison between the reverberation time and the existing parameters in terms of sensitivity to inter-turn short circuits confirms the advantages of the proposed approach.

The paper is organized as follows. In section 2, an overview of most significant methods and statistical parameters used for PT diagnostics is given. In section 3, the procedure for calculating the reverberation time is explained. The experimental setup is described in section 4. The results obtained using the SFRA analyzer and the audio card are displayed in section 5. Conclusions of the research are derived in section 6.

2. Background theory

This section provides an overview of the basic theoretical knowledge and definitions of the most significant SFRA indicators. Mechanical failures of PT are caused by a variety of internal and external conditions. These failures are very progressive and can be detected by analyzing the winding response to an input signal containing a wide range of spectral components. When injecting the input signal in the PT terminal, the PT response, i.e., the output signal, is measured. There are different possible measurement schemes: End-to-end (source to phase terminal), End-to-end (source to neutral terminal), End-to-end short-circuit (source to phase terminal), End-to-end short-circuit (source to neutral terminal), Capacitive inter-winding and Inductive inter-winding. In these measurements, the winding of a PT can be viewed as a two-port network comprising resistors, capacitors, and inductors, where the resistance is normally negligible. The result of the FRA method is a response that is represented on a logarithmic scale. If the two compared frequency responses do not differ, it means that the longitudinal parameters have not changed significantly, i.e., there were no winding deformations since the previous measurement. In the case of mechanical winding defects, the values of equivalent capacitors and inductors are changed, and the responses of two periodic tests differ, which indicates defect.

Interpretation of FRA results is performed empirically based on images generated by specialized devices. In many tests, it is not enough to observe only the frequency response, but the transfer functions for each test are calculated. First, the input and output signal are recorded, after which the Fourier transform is performed on the recorded signals:

$$F(j\omega) = \int_{-\infty}^{\infty} e^{-j\omega t} f(t)\, dt \tag{1}$$

where $f(t)$ is the time-domain form of the recorded signal. The impulse response in the frequency domain $H(j\omega)$ is formed as the ratio of the response (output) V_{output}, and source (input) V_{input} signal:

$$H(j\omega) = \frac{V_{output}(j\omega)}{V_{input}(j\omega)} \tag{2}$$

The amplitude characteristic is most used for the analysis. The ordinate represents the amplitude of the transfer function in decibels and the abscissa represents the frequency on a logarithmic scale. This approach with the transition to the frequency domain greatly facilitates the analysis and provides independence from the waveform of the excitation. By comparing the calculated transfer functions in successive tests, different changes in the winding geometry and changes in the PT magnetic circuit can be detected. Interpretation of the SFRA results relies on personal expertise and can lead to different conclusions. It is not possible to draw clear conclusions about the failure based on the visual comparison of two diagrams. Moreover, the conventional SFRA fingerprint is very inaccurate in detecting incipient and low mechanical fault levels [12]. In order to resolve these problems, various statistical indicators are proposed [6,11,12,13]. These indicators can be divided into two categories: those extracted directly from SFRA amplitude characteristic and those based on the resonance and anti-resonance points. These indicators are summarized and presented in Table 1. A sensitivity analysis of these indicators can be performed by calculating their values for different fault intensities, i.e., short circuits across different portions of the winding. This analysis will be presented in section 5.

3. Impulse response and reverberation time

In digital signal processing theory, a linear time-invariant (LTI)

Table 1
Statistical indicators obtained from SFRA results (N – overall size of the data set; x_i and y_i – samples of the input and output signal; $\overline{x}$ and $\overline{y}$- mean values).

Indicator	Description
Jaccard Distance (JD)	$JD = \frac{\sum_{i=1}^{N}(x_i - y_i)^2}{\sqrt{\sum_{i=1}^{N}(x_i-\overline{x})^2\sum_{i=1}^{N}(y_i-\overline{y})^2}}$
Absolute sum of logarithmic error (ASLE)	$ASLE = \frac{\sum_{i=1}^{N}\lvert 20log_{10}(y_i) - 20log_{10}(x_i)\rvert}{N}$
Absolute average difference (DABS)	$DABS = \frac{\sum_{i=1}^{N}\lvert y_i - x_i\rvert}{N}$
Min–max ratio (MM)	$MM = \frac{\sum_{i=1}^{N}min(y_i,x_i)}{\sum_{i=1}^{N}max(y_i,x_i)}$
Sum Squared Max-Min Ratio Error (SSMMRE)	$1 - SSMMRE = 1 - \frac{1}{N}\frac{\sum_{i=1}^{N}min(y_i,x_i)}{\sum_{i=1}^{N}max(y_i,x_i)}$
Least Squared Error (LSE)	$LSE = \frac{\sum_{i=1}^{N}(x_i-\overline{x})(y_i-\overline{y})}{\sum_{i=1}^{N}(x_i-\overline{x})^2}$
Sum of Error (SE)	$SE = \frac{\sum_{i=1}^{N}(y_i - x_i)}{N}$
Variance (Var)	$\sigma^2 = \frac{\sum_{i=1}^{N}(y_i - \overline{x})}{N}$

system can be unambiguously described by its frequency response or the impulse response in the time domain [19]. The frequency response of a system is obtained by applying the Fourier transform to the impulse response in the time domain, according to (1). The impulse response can theoretically be obtained by exciting the system with a Dirac impulse. However, generating a Dirac impulse is not possible in practice, therefore a unit pulse or Heaviside step signal are used instead. More frequently, indirect methods such as the sweep (chirp) signal and the MLS sequence method are employed [20]. The impulse response is commonly used in the areas of signal processing, automatic control, acoustics, etc. The impulse response has become extensively used in acoustics (most notably room acoustics) due to the development of computers which allowed simple and efficient calculation and display of the impulse response.

The impulse response of a room is measured using a speaker and microphone. The room can be viewed as an LTI system, where the microphone signal represents the system output and the signal emitted from the speaker represents the system input. The impulse response of a room represents its “ID”, as it allows all acoustic parameters of the room to be determined. An example of an impulse response of a room is shown in Fig. 1 (a). The structure of the impulse response is very complex, and its waveform does not provide much information about the room. The sound field in the room can usually be analyzed simply by observing the global form of the envelope of the impulse response, i.e., the rate of the sound level reduction. Therefore, the impulse response is most often characterized by the so-called sound decay curve, commonly referred to as the “reverberation curve” [18]. The reverberation curve is obtained by calculating the sound level of the response signal averaged over a selected interval. To reduce the influence of fluctuations of the reverberation curve, the so-called integrated impulse response, also known as the “Schroeder curve” is often employed [18]. This approach is based on introducing the decay curve $L_R(t)$, defined as:

$$L_R(t) = \int_t^{\infty} h^2(t)dt = \int_0^{\infty} h^2(t)dt - \int_0^{t} h^2(t)dt \tag{3}$$

where $h(t)$ is the impulse response of the system. Fig. 1 (b) displays the reverberation curve of the impulse response shown in Fig. 1 (a). The most used parameter obtained from the Schroeder curve is the reverberation time, denoted by T60. The reverberation time is defined as the time required for the reverberation curve to reduce by 60 dB from its initial value, which corresponds to a decrease of one million times on a linear scale. It can be considered that no sound energy remains in the room after the reverberation time has passed. The dynamic range of 60 dB is difficult to achieve in practice, which is why T60 is determined indirectly using parameters T10, T20, or T30. The interpretation of these parameters is illustrated in Fig. 1 (b) [18]. The reverberation time T60 is calculated by multiplying T30 by two, T20 by three, or T10 by six.

The possibility of using the reverberation time T60 as an indicator for determining the condition of a PT is examined in this paper. Unlike room acoustics, where the excitation and the impulse are acoustic signals (sound pressure), the excitation and impulse response of a PT are electric signals (voltage). Even though the measured quantities are different in nature, the principle of calculating the reverberation time is equally valid in both physical domains. In a more general sense, the reverberation time can be interpreted as a settling time of an impulse response, i.e., the time required for an impulse response to reduce to a negligibly small value.

4. The experimental setup

The experimental setup is schematically displayed in Fig. 2. The PT used in the setup was specially manufactured in the Laboratory for High Voltage at the University of Belgrade. The nameplate parameters of the PT are: rated voltage 10/0,4 kV/kV, rated current 23/557 A/A, frequency 50 Hz, connection type Ynyn0, and number of phases 3. This PT has seven sets of double cake windings with accessible taps on the phase W winding, labeled 0–7 in Fig. 2. Such a construction allows short-circuiting different portions of the winding. Depending on the connections between these terminals, the fault degree can be varied, with short circuits between adjacent taps corresponding to the smallest, and the short circuit between taps 0 and 7 corresponding to the largest fault degree. The phase W winding is excited using a variable-frequency source (blue line). The input voltage (u_1) is measured between the

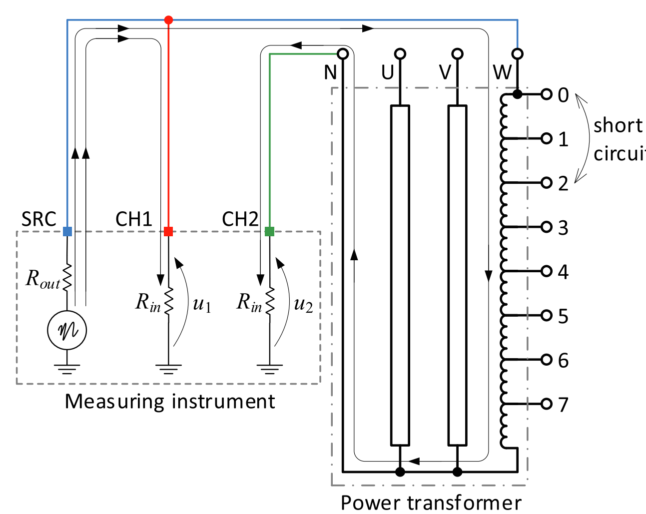

Fig. 2. Schematic display of the experimental setup (only the primary winding of the transformer is displayed).

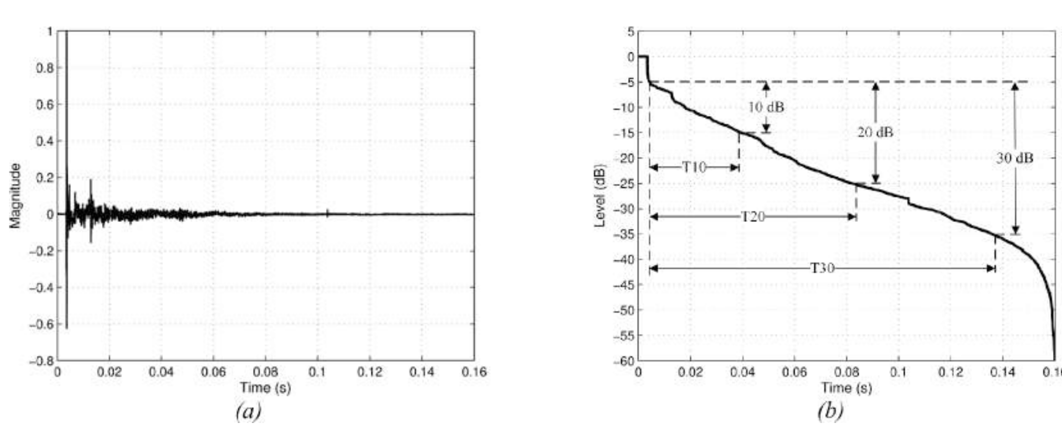

Fig. 1. Determination of reverberation time for an example room: (a) Impulse response, (b) Reverberation curve and definition of T10, T20, and T30.

phase W terminal and the ground (Channel 1 – red line). The voltage corresponding to the response (u_2) is measured between the transformer neutral point and the ground (Channel 2 – green line). Based on these two measurements, the frequency response of the winding can be obtained. The current paths are denoted using black lines with arrowheads.

The connection diagram of Fig. 2 is valid regardless of the applied instrument. Depending on the specific testing method and equipment, the block denoted "Measuring instrument" represents either the Doble M5400 SFR Analyzer or a sound card. A total of eight measurements were performed using each instrument, one on a healthy PT (denoted OK) and seven on a faulty PT (denoted SC). The fault was inflicted by creating a short circuit between tap 0 and taps 1 through 7 (see Fig. 2) to analyze faults of different severity. The logarithm frequency sweep signal was used as an excitation with both devices.

The first set of measurements was performed using the Doble M5400 SFR Analyzer [21]. This analyzer is used to provide a frequency response measurement in the range from 20 Hz to 2 MHz and represents a standard instrument for these types of measurements. The time required to obtain an individual measurement using this instrument is around 2 min.

The second set of measurements was performed using the Steinberg UR22 Sound Card [22]. This device represents an external audio card normally used for recording audio signals. The price of the device is around 150 $, several orders of magnitude lower compared to a professional SFR analyzer. The time required to acquire a single measurement is less than 10 s. The maximal sampling frequency of the Sound Card is 192 kHz, limiting the bandwidth of the measured signal to 96 kHz. Therefore, this device enables frequency response measurement in the range from 20 Hz to roughly 100 kHz.

The professional SFR Analyzer is used to clearly establish the benefit of the new indicator (reverberation time) compared to the existing mathematical indicators. The idea behind using the audio card is to examine the possibility of using this device for SFRA and for obtaining the proposed fault indicator (reverberation time). The first set of measurements is used as a reference. The second set of measurements is compared to the first set to determine if the low-cost sound card is applicable for detecting PT winding faults and quantifying their severity.

5. Results and discussion

5.1. Results obtained using the Doble M5400 SFR Analyzer

The frequency responses of the PT with a healthy winding (blue) and with inter–turn short circuits (other colors) are shown in Fig. 3. The given responses were obtained according to (2) using the Doble M5400

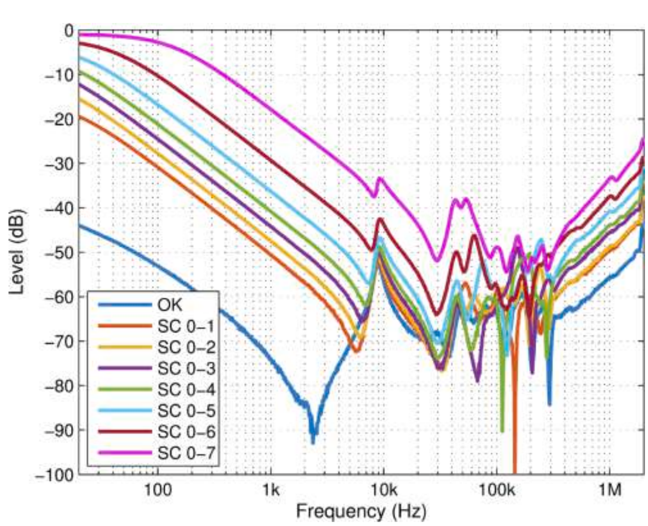

Fig. 3. Frequency responses obtained using the SFR Analyzer.

SFR Analyzer (referred to as "SFR Analyzer" from here on in), based on measured input and output voltages u_1 and u_2, as shown in Fig. 2. An increased level of the frequency response is observed when the inter-turn faults are present, which can be attributed to the variation of winding parameters (inductances and capacitances).

The most pronounced increase of up to 50 dB is observed in the low-frequency region, below 2 kHz. The PT can be treated as a complex RLC network, with inter–turn short circuits affecting the equivalent impedance of the winding [23]. This effect is the most pronounced at low frequencies, where the winding inductances are dominant. The reduction of winding impedance leads to an increase of voltage on CH2 (Fig. 2), thereby increasing the frequency response. As the severity of the fault, i.e., the number of short-circuited turns, increases, so does the level of the frequency response. The resonant frequency retains its value of around 10 kHz regardless of the winding condition. The increase of the frequency response in the high–frequency region, where the PT behaves mostly as a capacitive network, is less pronounced, and does not exceed 30 dB. By observing the low-frequency portion of transfer functions for different faults of observed PT given in Fig. 3, it can be noted that the transfer function of the lowest magnitude corresponds to a healthy transformer (OK state), and as the severity of the fault increases (from SC 0–1 to SC 0–7) the transfer function magnitude increases as well. However, the overlap between transfer functions in the high–frequency region and their proximity in the low–frequency region make it difficult to unambiguously determine the fault severity. Various statistical indicators have therefore been proposed over the years. The most significant ones are presented below.

The frequency responses of Fig. 3 were obtained using the measured signals from channel 1 (excitation) and channel 2 (response) of the SFR Analyzer. Based on these signals, statistical indicators defined in Table 1 are calculated. The calculated values are plotted in Fig. 4 for all analyzed winding conditions.

The values of the Jaccard Distance (JD) are given in Fig. 4 (a). This indicator is equal to 0 for a healthy PT, and ranges from −0.13 to 0.25 when inter-turn short circuits are present. Therefore, this parameter is not suitable for determining the winding condition, nor can it indicate the severity of the fault, i.e., the number of short-circuited turns. Similar conclusions hold for the Sum of Error and Variance parameters shown in Fig. 4 (g) and (h). The values of the Least Squared Error (LSE) indicator are plotted in Fig. 4 (f). This parameter is of approximately equal value when the winding is healthy and when the least severe fault (SC 0–1) is present. On the other hand, the values of LSE decrease monotonically for more severe faults (SC 0–2 to SC 0–7). This indicator can therefore be used for detecting the presence and degree of inter-turn short-circuits, but only if significant portions of the winding are short-circuited. It should be noted that the sensitivity of the LSE is rather low, as it decreases by only 25% for the most severe fault (SC 0–7) compared to the healthy state.

The indicators displayed in Fig. 4 (b), (c), (d), and (e), namely: Absolute sum of Logarithmic Error (ASLE), Absolute average difference (DABS), Min–max ratio (MM), and Sum Squared Max–Min Ratio Error (1–SSMMRE) clearly distinguish a healthy PT from a faulted one. The 1-SSMMRE indicator exhibits variations of only 6% and does not vary monotonically as the fault severity increases, making it difficult to determine the fault severity. The same holds for the MM indicator, except that its fault–induced variations are more pronounced compared to 1–SSMMRE, making it more suitable for fault detection.

ASLE and DABS change prominently when a winding fault is introduced, which enables very reliable fault detection. As visible from Fig. 4 (b) and (c), neither of the two indicators changes monotonically, and the fault degree can therefore not be confidently determined. Nevertheless, these two indicators have a clear advantage compared to other indicators shown in Fig. 4, as they provide the most reliable fault detection and can indicate fault severity to a certain extent.

The response of the system (winding) was calculated for each experiment based on the SFRA results (amplitude and phase

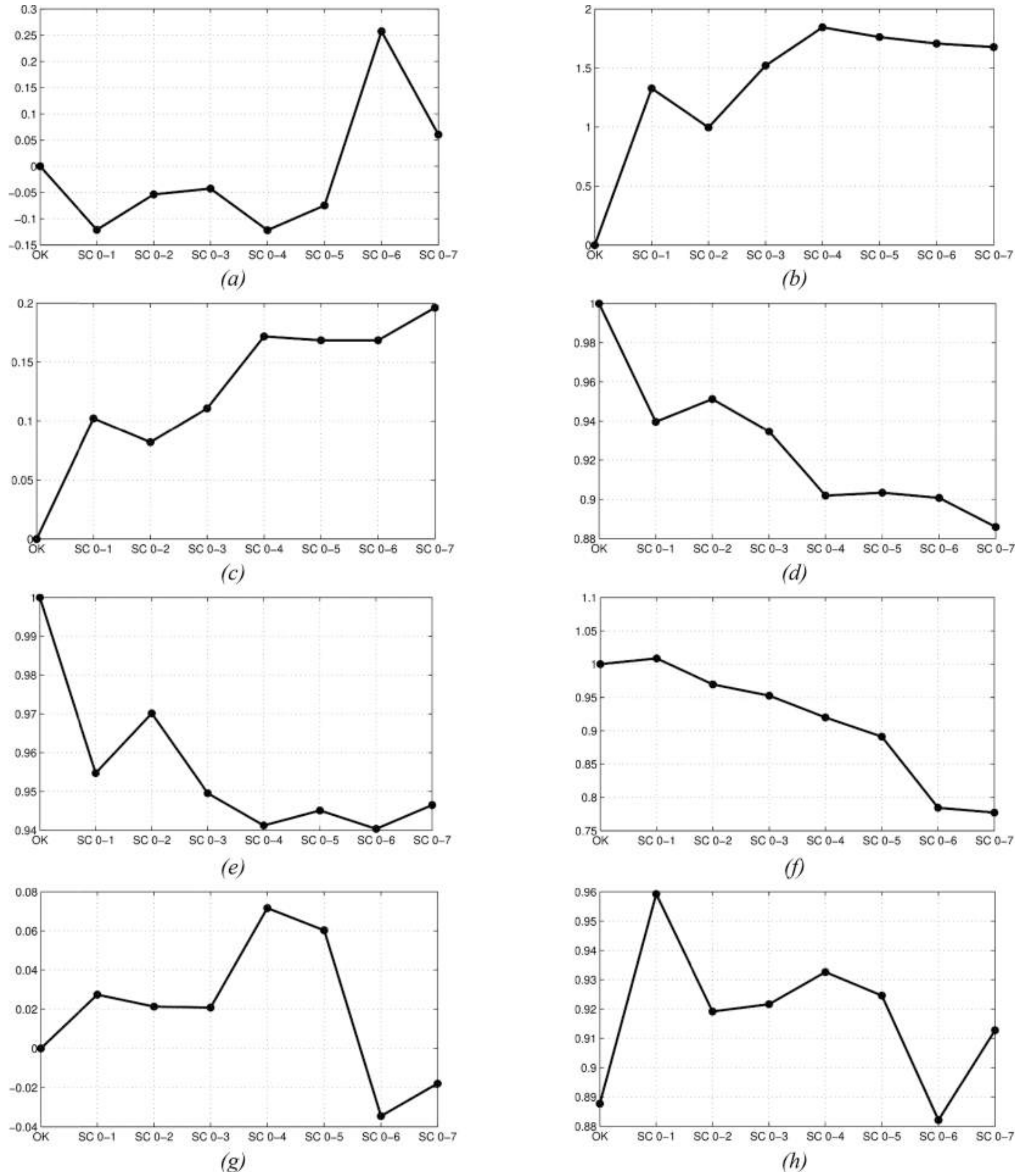

Fig. 4. Statistical indicators calculated based on Table 1: (a) Jaccard Distance (JD); (b) Absolute sum of logarithmic error (ASLE); (c) Absolute average difference (DABS); (d) Min–max ratio (MM); (e) Sum Squared Max-Min Ratio Error (1-SSMMRE); (f) Least Squared Error (LSE); (g) Sum of Error (SE); (h) Variance (Var).

characteristics) and the known waveform of the excitation signal. The signal level decay curves (reverberation curves) corresponding to all analyzed scenarios are obtained from (3) using the calculated impulse responses and are displayed in Fig. 5. All curves exhibit similar behavior over the first 10 ms. Following this interval, the curve corresponding to the healthy case exhibits a lower decay rate compared to those corresponding to the faulty PT. As the fault severity, i.e., the number of short-circuited turns, increases, so does the slope of the decay curves.

The reverberation time (T60) is calculated according to Fig. 2 (b). The dynamic range of 20 dB, i.e., the T20 parameter, was used to calculate T60. Dashed lines in Fig. 5 indicate levels of –5 dB and –25 dB used to calculate T20. The reverberation time values obtained for the healthy PT and the analyzed fault conditions are displayed in Fig. 6. The value of T60 for a healthy PT is 508 ms. When the least severe fault (SC 0–1) is present, T60 reduces to 161 ms, which is a 70% decrease compared to the healthy state. The values of T60 range from 7 ms for the most severe fault (SC 0–7) to 139.5 ms for SC 0–2. The significant decrease of T60 when a fault is introduced enables very reliable fault detection. Furthermore, T60 decreases monotonically as the extent of the inter–turn short circuit increases. On the other hand, none of the indicators shown in Fig. 4 exhibits strictly monotonous variation as fault severity increases, and only ASLE and DABS (Fig. 4 (b) and (c)) enable reliable fault detection due to their abrupt change when a fault is introduced. This gives the proposed parameter a distinct advantage over the existing SFRA-based parameters in terms of its ability to clearly indicate fault severity.

5.2. Results obtained using SFR Analyzer – Reduced frequency range

By observing the frequency responses shown in Fig. 3 it becomes apparent that the energy is mostly contained in the low-frequency region, the energy being proportional to the square of the response amplitude. This is particularly notable in fault conditions, when the highest values of the response amplitude are located under 10 kHz, which is well below the bandwidth limit of 2 MHz. The reverberation time T60 represents the time required for the impulse response of the PT

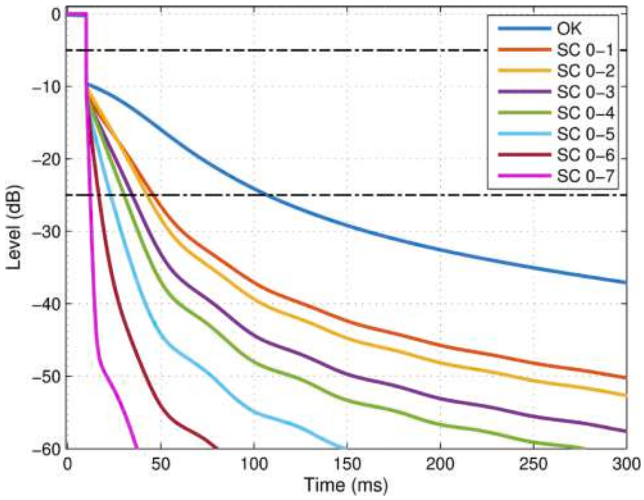

Fig. 5. Reverberation curve obtained using the SFR Analyzer.

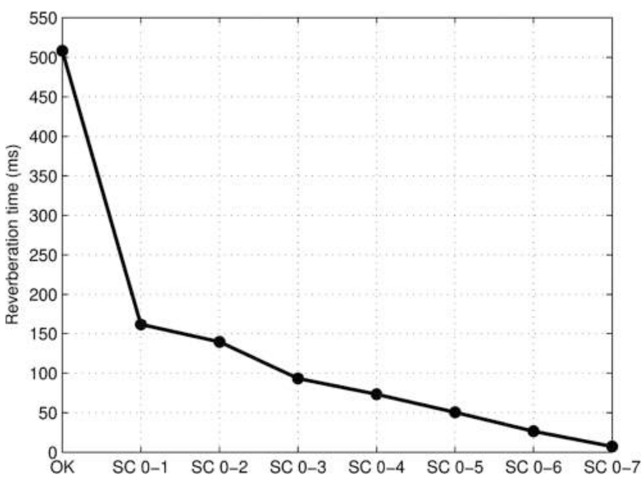

Fig. 6. Parameter T60 obtained using the SFR Analyzer.

to diminish. As most of the energy is contained in the at lower frequencies in all analyzed cases, the low-frequency components will dictate the reverberation time. It is therefore assumed that recording a signal using an SFR analyzer with a lower bandwidth will not influence the value of T60 significantly. Reducing the frequency range of the SFRA would not only simplify the measuring procedure, but would also reduce the time required for measurement and signal processing. To verify this assumption, digital filtering of the response and recalculation of T60 was performed for all experiments. Three reduced frequency ranges were used, with upper limits of 1 MHz, 500 kHz and 100 kHz. Table 2 shows the frequency response energies corresponding to these ranges as a percentage of the energy corresponding to the full range of 2 MHz. The results are given for healthy conditions and for a fault of medium severity (SC 0–4). The energy content for the original bandwidth (2 MHz) is 100%. When the frequency range is halved, 75.9% of the total energy is preserved with a healthy PT, whereas a reduction of merely 3% is observed with a faulty PT. Reducing the frequency range 20 times leads to a reduction in energy of 50% in the case of a healthy PT and only 6% in the case of a faulty PT. A significant amount of energy is preserved despite the drastic reduction of the frequency range, especially when an inter-winding short circuit is present. It is therefore justified to expect that the reverberation time will not vary considerably due to filtering.

Table 2
Ratio of frequency response energy in the reduced range to the energy in the full (2 MHz) range.

Frequency range (MHz)	Healthy PT (%)	Faulty PT (SC 0–4) (%)
1	75.9	96.7
0.5	66.8	95.4
0.1	56.8	94.2

The values of reverberation time obtained for all analyzed conditions and different frequency ranges (full and reduced) are shown in Fig. 7. The values of T60 are somewhat higher for the reduced ranges compared to the original range of 2 MHz in all conditions, with the least pronounced deviations when the PT is under severe fault conditions. Nevertheless, the trend of T60 is unchanged compared to the original range. This means that the value of T60 obtained using signals in a reduced frequency range is a reliable indicator of the presence and severity of an inter-turn short circuit. Therefore, if reverberation time is used as a fault indicator, the frequency range of SFRA can be reduced, which results in less time-consuming measurement and signal processing procedures. Additionally, the complexity and price of the instrument itself can be reduced significantly when a lower sampling frequency is required. It is worth noting that reverberation time calculated at a reduced frequency range retains its advantages compared to the existing indicators listed in Table 1.

5.3. Results obtained using the Sound Card

It was shown in the previous subsection that the reverberation time can be used as a fault indicator even if the frequency range of measured signals is well below 2 MHz offered by the professional SFR Analyzer. Therefore, a second group of experiments was conducted using a Steinberg UR22 Sound Card with a frequency range of approximately 100 kHz. As with SFR Analyzer, a frequency sweep signal was used as the excitation. The frequency range of the sweep signal was between 20 Hz and 100 kHz. Based on the measurements from channels 1 and 2 (see Fig. 2) the impulse responses are obtained for the same PT conditions as in the first group of measurements.

Based on (3) and the recorded impulse responses, the signal level decay curves are calculated. The decay curves corresponding to the healthy PT and the six analyzed fault conditions are displayed in Fig. 8. These curves have a somewhat different trend compared to those obtained using the SFR Analyzer (Fig. 5), which is expected due to the significantly lower bandwidth of the Sound Card. However, the slope of the decay curves is the approximately the same in the amplitude range of interest regardless of the employed instrument. As the parameter T60 is directly dependent on the slope of the decay curve, it is reasonable to expect the reverberation time obtained using the Sound Card to be

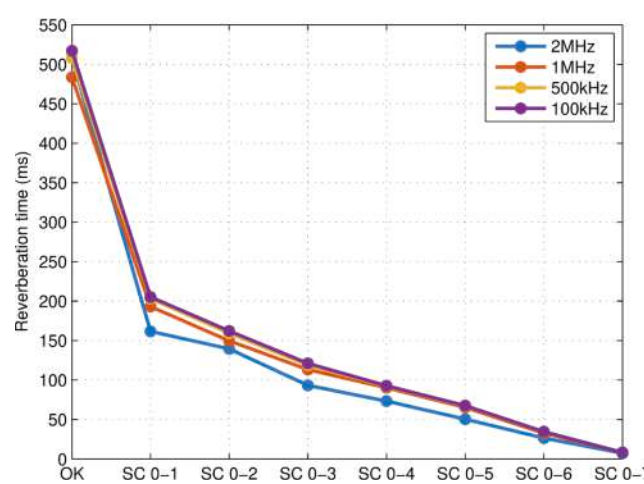

Fig. 7. A comparison between the values of T60 obtained using SFR Analyzer for different frequency ranges.

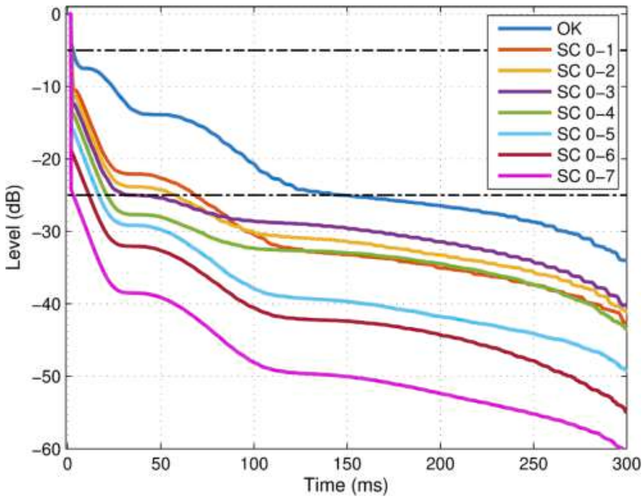

Fig. 8. Reverberation curve for Sound card.

approximately equal to that obtained using the SFR Analyzer.

According to Fig. 9, the value of reverberation time in the case of a healthy PT is 434 ms, whereas for the fault of lowest severity (SC 0–1) it decreases to 198 ms. The value of T60 further reduces as the number of short-circuited turns increases. Therefore, the value of T60 obtained using the Sound Card measurements enables reliable fault detection and determination of fault severity. For the sake of comparison, the values of T60 obtained using the SFR Analyzer are plotted in Fig. 9 as well. The two sets of values differ the most when the PT is healthy or when the fault is of low severity (SC 0–1 and SC 0–2). Even though certain discrepancies exist, the trend of T60 remains the same regardless of the employed instrument. Therefore, the fault detection capability also remains unchanged, despite the far lower frequency range of the Sound Card.

The Sound Card is advantageous compared to the SFR Analyzer in terms of individual measurement duration – 5 s using the Sound Card compared to 2 min using the SFR Analyzer. Another advantage of the Sound Card is its simpler design due to lower bandwidth, and consequentially a much lower price compared to any professional SFR analyzer. By conducting the SFR analysis and calculating the proposed indicator (reverberation time T60) using the Sound Card, reliable fault detection and quantification can be performed. The results given in this paper clearly demonstrate that applying the proposed procedure using a simple audio instrument ensures unambiguous fault indication.

6. Conclusion

Reverberation time (T60) is introduced in this paper as a new parameter for PT fault detection. Although used predominantly in room acoustics, reverberation time, in a more general sense, represents the settling time of an impulse response. A major advantage of this parameter is that its calculation requires only the time–domain waveforms of input and response signals, rather than their frequency-domain representations, which makes the calculation procedure simple and efficient. The reference measurements obtained using a professional SFR Analyzer prove the capability of the new parameter to indicate the presence and severity of an internal winding fault. Additionally, the new parameter has an advantage over existing statistical SFRA-based indicators, especially in terms of determining the fault severity.

The new parameter T60 was recalculated for different frequency ranges below the standard 2 MHz provided by the professional SFR Analyzer. The obtained results demonstrate that T60 calculated at a reduced frequency range still enables reliable fault detection and quantification, even when the range is reduced by as much as 20 times compared to the original 2 MHz. The possibility of narrowing the measurement channel bandwidth can reduce the overall experiment duration due to shorter signal acquisition and processing time. Additionally, the complexity and cost of the instrument can also be reduced significantly.

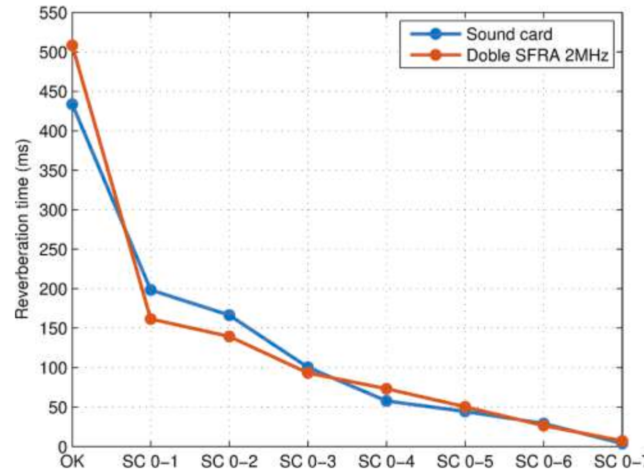

Fig. 9. Comparison Reverberation time T60 obtained using the Sound Card and the SFR Analyzer.

A second set of experiments employing a Sound Card with the upper frequency limit of approximately 100 kHz was conducted. This instrument does not comply with the standard demands for SFRA due to its low bandwidth. However, the values of T60 obtained using this instrument exhibit very small deviations compared to the ones obtained using the SFR Analyzer. Therefore, the use of the Sound Card ensures fault detection and quantification of equal reliability as that achieved using the SFR Analyzer. Considering its simpler design, significantly lower cost, and shorter time required for measurement and signal processing, the Sound Card represents a very beneficial alternative to professional SFR analyzers for preliminary PT diagnostics.

Future work will be focused on using the reverberation time T60 for detecting other types of internal PT faults, such as winding deformations. The possibility of using the proposed parameter to monitor PT ageing will be examined as well.

CRediT authorship contribution statement

Milos Bjelić: Formal analysis, Methodology, Software, Visualization. **Bogdan Brković:** Investigation, Writing – original draft, Writing – review & editing. **Mileta Žarković:** Supervision, Conceptualization. **Tatjana Miljković:** Software, Writing – original draft.

Declaration of Competing Interest

The authors declare that they have no known competing financial interests or personal relationships that could have appeared to influence the work reported in this paper.

Acknowledgment

The authors would like to thank the Ministry of Education, Science and Technological Development of the Republic of Serbia which, within the framework of Project III 42009 'Smart grid' and Project TR36026, made this work possible. We would like to express special appreciation to Mr. Denis Ilic for his help in conducting the SFR Analyzer measurements.

References

[1] Ghani SA, Thayoob YHM, Ghazali YZY, Khiar MSA, Chairul IS. Condition monitoring of distribution transformer's mechanical parts using sweep frequency response analysis (SFRA). Procedia Eng. 2013;68:469–76.

[2] Kornatowski E, Banaszak S. Diagnostics of a transformer's active part with complementary FRA and VM measurements. IEEE Trans. Power Delivery 2014;29 (3):1398–406.

[3] IEEE PC57.149/D8, Guide for the Application and Interpretation of Frequency Response Analysis for Oil Immersed Transformers, 2012.

[4] IEC 60076-18, Power transformers - Part 18: Measurement of frequency response,2012.

[5] CIGRE Working Group A2.26, "Mechanical-condition assessment of transformer windings using frequency response analysis", 2008.

[6] CIGRE Working Group A2,53 "Advances in the interpretation of transformer Frequency Response Analysis (FRA)", Reference 812, September, 2020.

[7] Secue JR, Mombello E. Sweep frequency response analysis (SFRA) for the assessment of winding displacements and deformation in power transformers. Electr. Power Syst. Res. 2008;78(6):1119–28.

[8] Abbasi A, Mahmoudi M. Diagnosis and clustering of power transformer winding fault types by cross-correlation and clustering analysis of FRA results. IET Gener. Transm. Distrib. 2018;12:4301–9.

[9] Pandya A, Parekh B. Interpretation of sweep frequency response analysis (SFRA) trace for the open circuit and short circuit winding fault damages of the power transformer. Int. J. Electr. Power Energy Syst. 2014;62:890–6.

[10] Sun J, Yang Q, Su P, Wu S, Chen S, He L. Diagnosis of winding fault in three-winding transformer using lightning impulse voltage. Electr. Power Syst. Res. 2019;175:105898. https://doi.org/10.1016/j.epsr.2019.105898.

[11] Behjat V, Vahedi A, Setayeshmehr A, Borsi H, Gockenbach E. Sweep frequency response analysis for diagnosis of low level short circuit faults on the windings of power transformers: An experimental study. Int. J. Electr. Power Energy Syst. 2012;42(1):78–90.

[12] Abbasi AR, Mahmoudi MR. Application of statistical control charts to discriminate transformer winding defects. Electr. Power Syst. Res. 2021;191:1–11.

[13] Khalili Senobari R, Sadeh J, Borsi H. Frequency response analysis (FRA) of transformers as a tool for fault detection and location: A review. Electr. Power Syst. Res. 2018;155:172–83.

[14] Shamlou A, Feyzi MR, Behjat V. Winding deformation classification in a power transformer based on the time-frequency image of frequency response analysis using Hilbert-Huang transform and evidence theory. Int. J. Electr. Power Energy Syst. 2021;129:1–15.

[15] Secue JR, Mombello EE. New SFRA measurement interpretation methodology for the diagnosis of power transformers. Electr. Eng. 2014;96(2):183–98.

[16] Ahmadi H, Vahidi B, Nematollahi AF. A simple method to detect internal and external short-circuit faults, classify and locate different internal faults in transformers. Electr. Eng. 2014;96:183–98.

[17] Zhao Z, Tang C, Chen Yu, Zhou Qu, Yao C, Islam S. Interpretation of transformer winding deformation fault by the spectral clustering of FRA signature. Int. J. Electr. Power Energy Syst. 2021;130:106933. https://doi.org/10.1016/j.ijepes.2021.106933.

[18] Schroeder MR. New method of measuring reverberation time. J. Acoust. Soc. Am. March 1965;37(6):409–12. https://doi.org/10.1121/1.1909343.

[19] A Papoulis, Circuits and Systems: A Modern Approach, Oxford University Press. June 8, 1995.

[20] Stan GV, Embrechts JJ, Archambeau D. Comparison of different impulse response measurement techniques. J. Audio Eng. Soc. April 2002;50(4):249–62.

[21] Technical documentation of Doble M5400 SFRA Analyzer, available at: https://www.doble.com/product/m5400/, accessed on June 19th 2021.

[22] Technical documentation of Steinberg UR22 Sound Card, available at http://download.steinberg.net/downloads_hardware/UR22/UR22_documentation/UR22_OperationManual_en.pdf, accessed on June 19th 2021.

[23] Zhao X, Yao C, Abu-Siada A, Liao R. High frequency electric circuit modeling for transformer frequency response analysis studies. Int. J. Electr. Power Energy Syst. 2019;111:351–68.